

Photocatalytic C–H Thiocyanation of Corroles: Development of Near-Infrared (NIR)-Emissive Dyes

Kasturi Sahu, Sruti Mondal, Shaikh M. Mobin, and Sanjib Kar*

Cite This: *J. Org. Chem.* 2021, 86, 3324–3333

Read Online

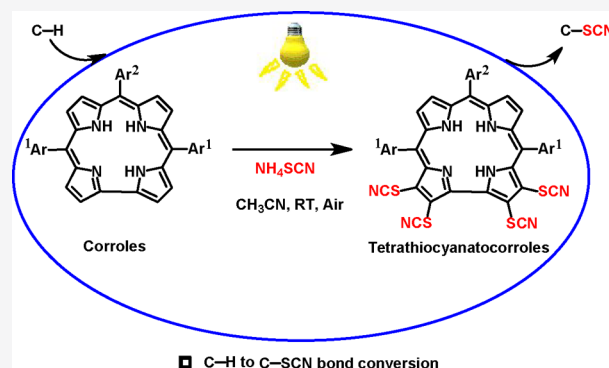
ACCESS |

Metrics & More

Article Recommendations

Supporting Information

ABSTRACT: A new method of activating corrole macrocycles via an *in situ* generated SCN radical has been developed at very mild conditions at room temperature. This photoredox reaction resulted in the generation of tetrathiocyanatocorroles in good yields. The synthesis of tetrathiocyanatocorroles was never reported earlier. Single-crystal XRD analysis reveals that the insertion of four thiocyanate moieties at the four β -pyrrolic positions has imparted significant distortion to the corrole macrocycle. The generated tetrathiocyanatocorroles are different from the parent corroles in many ways. The photophysical properties of the newly synthesized tetrathiocyanatocorroles are dramatically altered from the parent corroles. The absorption feature of these modified corrole derivatives (both position and intensity) bears a nice similarity with the chlorophyll-*a* macrocycle. Thus, these newly synthesized molecules can be considered as spectroscopic model systems for chlorophyll-*a* pigments. The observed absorption and emission spectra of these tetrathiocyanatocorroles certainly point out that these newly developed ligand scaffolds and their various metal complexes will have immense potential as pigments in solar cells and also as NIR-emissive dyes. The observed C-H...Au weak interactions in a representative Au(III)-corrole complex point out that these complexes are capable of activating the unfunctionalized C–H groups and thus will have potential implications in C–H activation reactions.



INTRODUCTION

Porphyrinoids are traditionally used as photosensitizers in singlet oxygen generation reactions.^{1–3} However, the applications of porphyrinoids in photoredox reactions are rather limited.^{4,5} Depending on the reaction conditions, the photoexcited triplet states of porphyrinoids can behave as either oxidant or reductant. A close comparison with the values of both ground state and excited state redox potentials of tetraphenylporphyrin reveals that, in the excited state, the porphyrinoids are more efficient electron donors and more efficient electron acceptors than in the ground state.⁶ Thus, porphyrinoids have great potential to replace the traditional photoredox catalysts like [Ru(bpy)₃]²⁺ and [Ir(ppy)₃] {bpy = bipyridine and ppy = 2-phenylpyridine}.^{7,8} Advantageously, the electronic and physicochemical properties of porphyrinoids can be fine-tuned by suitable functionalization at the periphery.⁹ Porphyrinoids, which will absorb the whole UV–vis region of the spectrum, will have great potential in this regard. Corrole, a contracted version of porphyrin having 18 π -electrons has many similarities with porphyrins.¹⁰ The spectroscopic properties of corroles are similar to those of porphyrin in many aspects.^{10–33} The triplet state lifetime of corroles is in the range of 10^{–4} to 10^{–5} s.¹⁰ Similar to porphyrin, corroles also act as a photosensitizer.^{34,35} Although there are few examples of porphyrin in photoredox catalysis,

similar studies in corroles are still rare. Herein, we have reported the application of corroles in a photocatalysis reaction. A unique reaction has been designed, in which corrole acts as a self-catalyst and introduces four thiocyanate groups in the β -pyrrolic positions and thus resulted in the formation of tetrathiocyanatocorroles. It is well-known that the thiocyanate motif is a potential building block in organic chemistry as it is the precursor of a host of sulfur-containing functional groups (e.g., sulfides, thioesters, and thiophenols) and also acts as a starting material of various heterocyclic compounds (e.g., thiazoles).^{36,37} Visible light-induced thiocyanation has recently gained ground to synthesize various thiocyanato appended arenes and heterocycles.^{38–40} Thus, these thiocyanato appended corroles will act as possible precursors for the synthesis of several sulfur-containing corrole derivatives and which will have potential implication in dyes and drugs. It was also observed that the β -substitutions at the

Received: November 10, 2020

Published: February 1, 2021



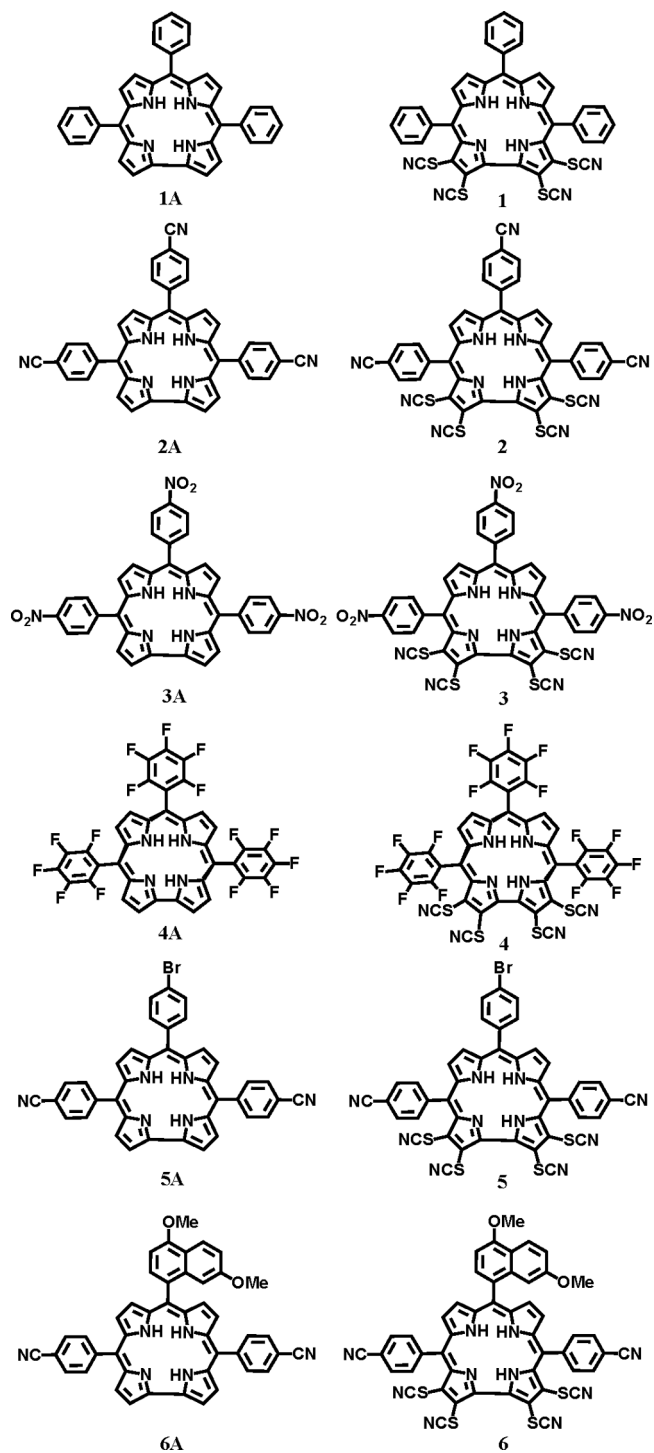
corrole ring has a pronounced effect on its electronic structure.^{41–45}

We have observed previously that, through ordinary chemical means, up to two thiocyanato groups can be inserted in the corrole periphery. The insertion of two thiocyanato groups in the corrole periphery was achieved in very drastic conditions and with low yields.⁴⁶ Although numerically it may not be a very big deal to insert four thiocyanato groups instead of two thiocyanato groups. However, to our ultimate surprise, we have observed that the photophysical properties are drastically altered in the case of tetrathiocyanatocorroles in comparison to dithiocyanatocorroles. In general, 18 π -electron systems like porphyrins and corroles have strong absorption in the 400–450 nm region, and also, they have much weaker absorption at around 500–650 nm (Q peaks).^{9,10} However, in the case of tetrathiocyanatocorroles, we have observed strong absorption in the whole visible region of the spectrum with a high molar absorption coefficient. To generalize this photochemical thiocyanation reaction, the substituents at the meso-phenyl rings of corroles are varied from electron-withdrawing groups (–CN [2A], –NO₂ [3A], –F [4A], and –Br [5A]) to electron-donating groups (–OMe [6A]) including the unsubstituted phenyl ring (–H [1A]). All the tetrathiocyanatocorroles were thoroughly characterized by several spectroscopic techniques. A representative example was also characterized by single-crystal XRD analysis. The present work thus describes the synthesis and characterization of six new tetrathiocyanatocorroles, namely, 2,3,17,18-tetrathiocyanato-5,10,15-triphenylcorrole, **1**; 2,3,17,18-tetrathiocyanato-5,10,15-tris(4-cyanophenyl)corrole, **2**; 2,3,17,18-tetrathiocyanato-5,10,15-tris(4-nitrophenyl)corrole, **3**; 2,3,17,18-tetrathiocyanato-5,10,15-tris(pentafluorophenyl)corrole, **4**; 2,3,17,18-tetrathiocyanato-10-(4-bromophenyl)-5,15-bis(4-cyanophenyl)corrole, **5**; and 2,3,17,18-tetrathiocyanato-10-(4,7-dimethoxynaphthalen-1-yl)-5,15-bis(4-cyanophenyl)corrole, **6** (Scheme 1). Four A₃-corrole and two *trans*-A₂B corrole have been chosen here as substrates to have the difference in energies of their molecular orbitals and thus having a difference in their photophysical properties. To explore the ability of these newly synthesized FB corroles {FB = free base} as potential ligand scaffolds, we have synthesized a new gold corrole complex, namely, {2,3,17,18-tetrathiocyanato-5,10,15-tris(4-cyanophenyl)corrolato-Au(III)}, **2-Au**. The corrolato-Au(III) complex, **2-Au**, was thoroughly characterized by several spectroscopic techniques including single-crystal XRD analysis.

RESULTS AND DISCUSSION

Synthesis and Characterization. Tetrathiocyanatocorrole derivatives (**1–6**) were synthesized by following a photocatalytic synthetic process developed by us. The corresponding free-base corroles (**1A–6A**) were dissolved in acetonitrile, and then excess NH₄SCN was added to it. The reaction mixture was stirred at room temperature under irradiation with a CFL lamp {CFL = compact fluorescent lamps} (20 W) for 5 h in the air, which resulted in the formation of tetrathiocyanatocorrole derivatives (**1–6**) in good yields (Scheme 2). Au(III) was inserted in the corrole cavity using gold acetate as a metal precursor in an acetonitrile and pyridine mixture at RT {RT = room temperature}. Purity and composition of the tetrathiocyanatocorrole derivatives (**1–6**) and the corrolato-Au(III) complex, **2-Au**, were established by their satisfactory elemental analyses, UV–vis, emission, IR,

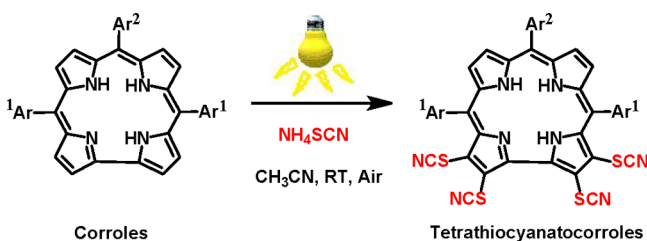
Scheme 1. Structures of the Corroles **1A–6A** and Their Corresponding 2,3,17,18-Tetrathiocyanatocorrole Derivatives **1–6**



NMR, and ESI-MS data and single-crystal XRD data (Figures S1–S46 and Tables S1–S3; see the Supporting Information).

A series of different solvents were screened to search for the most effective reaction media for these catalytic reactions. Polar solvents (as NH₄SCN is soluble in polar solvents) such as acetone, ethanol, THF {THF = tetrahydrofuran}, CH₃OH, DCE {DCE = 1,2-dichloroethane}, and 1,4-dioxane were screened for this purpose. We have observed that 2,3,17,18-tetrathiocyanatocorroles (**1–6**) were formed in trace amounts

Scheme 2. Synthetic Application of 2,3,17,18-Tetrathiocyanatocorroles



(yields < 1.0%) in THF and DCE solvents. Negligible yields (yields < 5.0%) were also obtained in CH₃OH and 1,4-dioxane medium. A yield of less than 10.0% was also obtained in acetone. A slight improvement in reaction yield was observed in the case of ethanol medium (yields < 15.0%). Alcohols, acetone, THF, 1,4-dioxane, and DCE are well-known free radical scavengers and thus lead to the destruction of *in situ* generated SCN radical, and as a result, they dictate the formation of 2,3,17,18-tetrathiocyanatocorroles (1–6). It is worthwhile to mention here that CH₃CN turns out to be the most effective solvent, and the reaction yields are consistently high with a value of as high as ~50.0%. We have observed that there are no traces of mono/di/tri-substituted corroles formed in most of the cases as side products in the optimized reaction conditions.

It was also observed that, in the absence of a CFL lamp, the reaction failed to deliver the desired product even after performing this reaction at room temperature and keeping all reactants, reaction conditions, and reaction time unchanged. This confirms that the light energy from a CFL lamp is necessary for this reaction, and it is a purely light-driven reaction. This reaction also failed to deliver the product in the absence of a thiocyanate source. NH₄SCN has turned out to be the best source of a thiocyanate group here.⁴⁷ It is possible to use KSCN as an alternate thiocyanate source; however, in

comparison to NH₄SCN, a 50% lowering of reaction yield was observed.

The ¹H NMR spectrum of 1 exhibits sharp peaks in the region δ , ~8.17–7.64 ppm; 2 exhibits sharp peaks in the region δ , ~8.09–7.74 ppm; 3 exhibits sharp peaks in the region δ , ~8.41–7.68 ppm; 4 exhibits sharp peaks in the region δ , ~7.93–7.66 ppm; 5 exhibits sharp peaks in the region δ , ~7.97–7.69 ppm; and 6 exhibits sharp peaks in the region δ , ~8.27–6.52 ppm. The peaks are shielded by ~0.8 ppm in the 2,3,17,18-tetrathiocyanatocorroles (1–6) corresponding to their starting FB corrole (1A–6A) analogues (see Supporting Information; Figures S34–S44). The ¹³C NMR spectrum of all these tetrathiocyanatocorrole derivatives shows their characteristic signals due to the presence of a SCN moiety at δ values of around ~111.0–112.0 ppm. The diamagnetic nature of the corrolato-Au(III) complex, 2-Au, is evident from its sharp resonances and having normal chemical shifts (Figures S45 and S46). The FT-IR spectra of 1–6 as KBr pellets show peaks at 2158, 2159, 2157, 2162, 2155, and 2156 cm⁻¹, respectively, due to strong S-CN stretching vibration (see Supporting Information; Figures S20–S25).

Crystal Structure. The crystal system of 2,3,17,18-tetrathiocyanatocorrole, 2, is triclinic in nature, and the unit cell has two molecules of 2. Although statistically four possible atropisomers can be obtained (based on the orientation of the SCN moieties at above (β) or below (α) the plane of the corrole ring), we have obtained only one atropisomer⁴⁸ ($\alpha_2\beta_2$ isomers) here (Figure 1 and Figure S1). Important crystallographic parameters for 2 are summarized in Table S1. Bond angles and distances of 2 tally well with the previously reported other FB corrole derivatives.¹⁰ The pyrrolic nitrogen atoms deviate from the 19-carbon atom mean corrole plane by distances ranging from 0.189 to (–0.149) Å in 2. The deviations observed in 2 are very much similar to those of the 5,10,15-triphenylcorrole (TPC). The corresponding deviations in TPC are 0.128–(–0.195) Å.⁴⁹ However, the dihedral angles

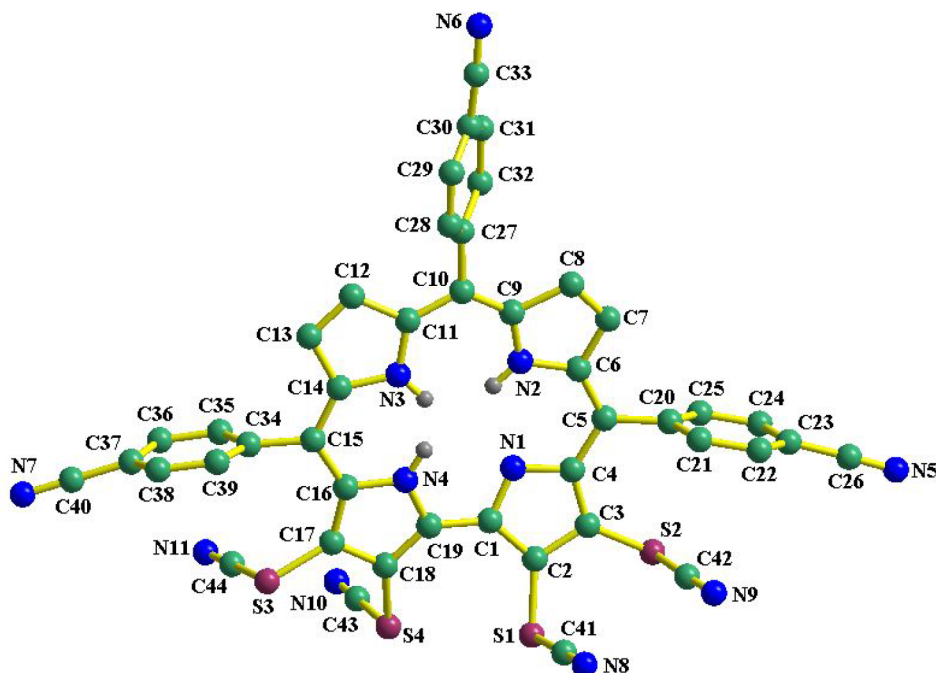


Figure 1. Single-crystal X-ray structure of 2. Hydrogen atoms are omitted for clarity.

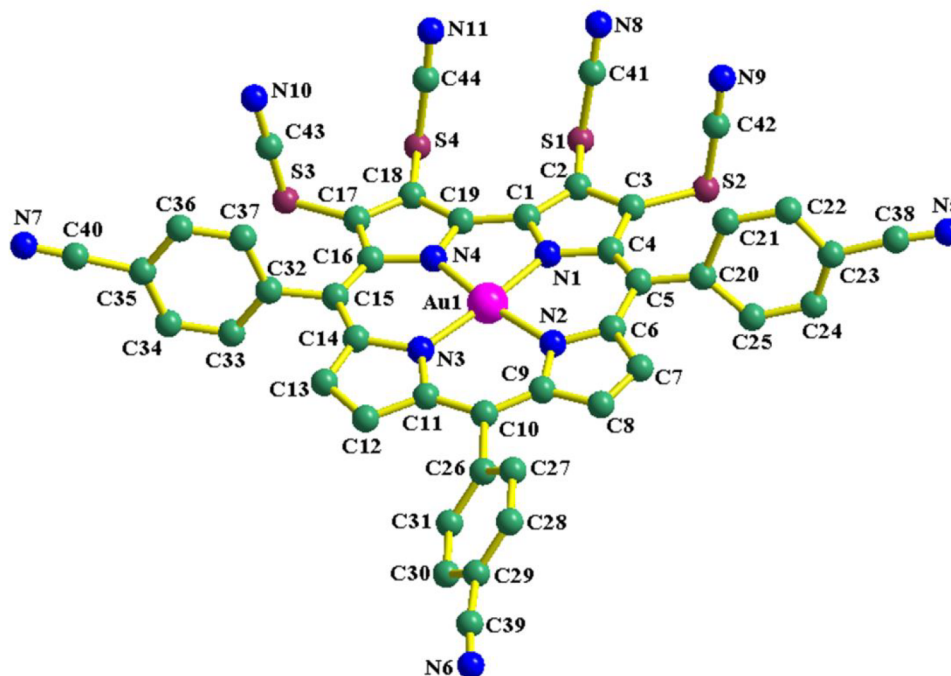


Figure 2. Single-crystal X-ray structure of 2-Au. Hydrogen atoms are omitted for clarity.

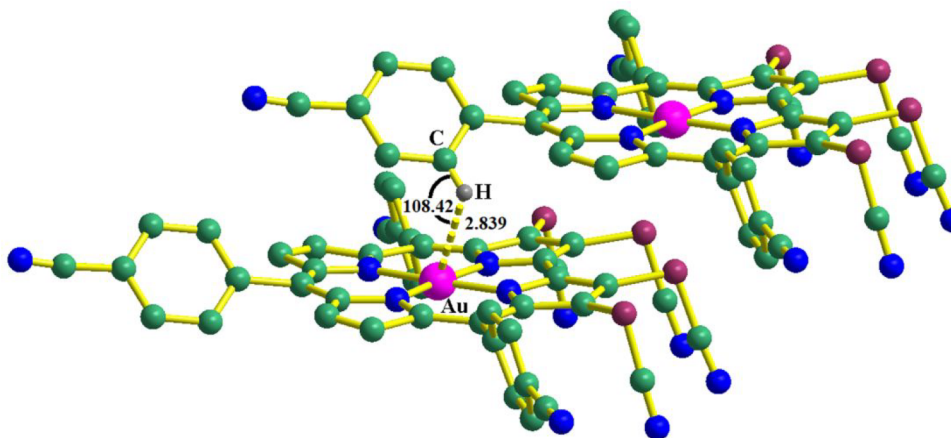


Figure 3. X-ray single-crystal structure analysis of 2-Au, showing C-H...Au interactions [$\angle\text{C-H}\cdots\text{Au} = 108.42^\circ$ and $\text{C-H}\cdots\text{Au} = 2.838 \text{ \AA}$] between neighboring molecules. The entry in square brackets is the angle and distance.

(between the planes of the *meso*-substituted phenyl rings and the 19-carbon mean corrole plane) in **2** differ significantly in comparison to the TPC. The dihedral angles in **2** are in the range of 63.64 – 85.46° , and the corresponding values in TPC are in the range of 41.74 – 50.33° .⁴⁹ Thus, the insertion of four thiocyanate moieties at the four β -pyrrolic positions (2, 3, 17, and 18) has imparted significant distortion to the corrole molecule, **2**.

The two thiocyanate groups are attached to each pyrrolic ring in *cis* fashion, but they are in *trans* orientation concerning the thiocyanate group attached with the neighboring pyrrole ring. The four $\text{C}\equiv\text{N}$ (derived from SCN unit) bond distances of **2** are in the range of 1.11 – 1.16 \AA , and the four $\angle\text{S}-\text{C}\equiv\text{N}$ bond angles are in the range of 176.47 – 179.07° (Figure 1).

The crystal system of {2,3,17,18-tetrathiocyanato-5,10,15-tris(4-cyanophenyl) corrolato-Au(III)}, **2-Au**, is monoclinic in nature, and the unit cell has four molecules of **2-Au**. In contrast to the FB 2,3,17,18-tetrathiocyanatocorrole, for **2-Au**, we have

obtained only the α_4 atropisomer. Important crystallographic parameters for **2-Au** are summarized in Table S2. Bond angles and distances of **2-Au** tally well with the previously reported other Au(III)-corroles.⁵⁰ The gold atom deviates from the mean N4 corrole plane by 0.0083 \AA (Figure 2 and Figure S2). The geometry around the gold center is not perfectly square planar.

The bite angles of N1-Au-N2 , N2-Au-N3 , N3-Au-N4 , and N4-Au-N1 are 90.81° , 94.23° , 93.69° , and 81.27° , respectively. The Au–N bond distances are in the range from 1.98 \AA for Au–N2 to 1.91 \AA for Au–N1 bonds and are slightly longer than those of a related Au(III) corrole.⁵¹ The pyrrolic nitrogen atoms deviate from the 19-carbon atom mean corrole plane by distances ranging from 0.0196 \AA to $(-0.0584) \text{ \AA}$. The dihedral angles in **2-Au** are in the range of 48.82 – 75.56° . X-ray single-crystal structure analysis of **2-Au** shows C-H...Au interactions between neighboring **2-Au** molecules, and it thus constitutes a rare example of C-H...Au interaction driven

supramolecular assembly formation in the gold chemistry (Figure 3). Earlier researchers have concluded that a significant strong C-H...Au interaction exists if the H...Au separation falls in the range of 2.3–3.0 Å, the C-H...Au angle falls in the range of 120–180°, and also an observable change noticed in the confirmation analysis.^{52–55} Herein, we have observed a H...Au distance of 2.838 Å and C-H...Au angle of 108.42°. The orientation of thiocyanate group also changes and resulted in the transformation of the $\alpha_2\beta_2$ atropisomer in corrole (2) to an α_4 atropisomer in the gold corrole (2-Au).

Electronic Absorption Spectroscopy. The electronic absorption spectra of tetrathiocyanatocorroles, 1–6, are shown in Figures S8–S13 (see the Supporting Information). The Soret band here is further split into at least three distinct bands, which thus indicates a lower symmetry compared to the FB corroles (Table S3, Figure 4, and Figures S8–S13). The

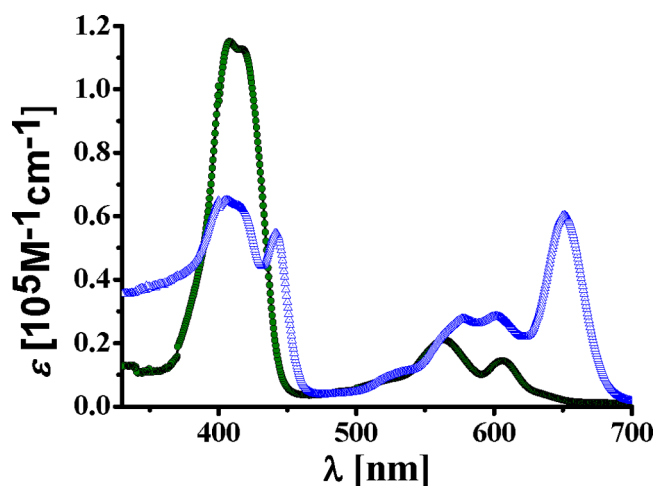


Figure 4. UV-vis absorption spectra of 5,10,15-tris(pentafluorophenyl)corrole, 4A (green line), and 2,3,17,18-tetrathiocyanato-5,10,15-tris(pentafluorophenyl)corrole, 4 (blue line), in acetonitrile.

most interesting phenomena are the appearance of at least four Q bands; out of them, the lowest energy band is as intense as the Soret bands. The Q bands in porphyrinoids are in general pseudoparity-forbidden and thus very weak.⁵⁶ Thus suitable external substitution can break this pairing property, and Q bands can be intensified. Unlike porphyrin and corroles, these absorption features of Q bands are fairly similar to the Q-type bands in the chlorophyll-*a* molecule. It was observed that the absorption feature of these modified corrole derivatives (both position and intensity) bears a nice similarity with the chlorophyll-*a* macrocycle.⁵⁷

Emission Properties. These tetrathiocyanatocorroles, 1–6, showed a significant red-shifted emission band compared to their parent corroles (1A–6A). The tail of the emission band reaches up to 850 nm (Figure 5, Figures S15–S19). These tetrathiocyanatocorrole derivatives (1–6) thus has the strong potential to become near-infrared (NIR)-emissive dyes. The obtained fluorescence quantum yields of 1–6 were estimated to be 0.07 for 1, 0.08 for 2, 0.11 for 4, 0.10 for 5, and 0.15 for 6, respectively. The low-lying singlet excited states of 1–6 are responsible for the origin of these kinds of emissive properties.¹⁰

Analysis of the Reaction Mechanism. To understand the reaction mechanism, several control reactions were performed (Figures S3–S7). To clarify if the reaction proceeds

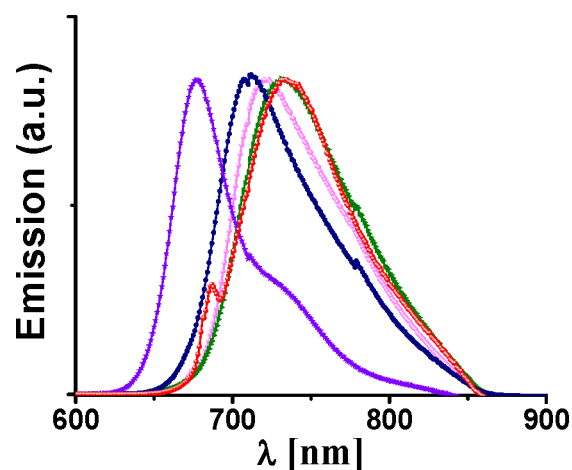


Figure 5. Normalized emission spectra of 2,3,17,18-tetrathiocyanatocorrole derivatives 1 (red line) in dichloromethane, 2 (navy blue line), 4 (violet line), 5 (magenta line), and 6 (olive green line) in acetonitrile.

via a radical pathway, we have used a radical inhibitor (see the Supporting Information for Mechanistic Studies). When 2.5 equiv of a commonly used radical inhibitor, like TEMPO {TEMPO = 2,2,6,6-tetramethyl-1-piperidinyloxy}, was used in the reaction mixture, we have not observed the formation of the desired 2,3,17,18-tetrathiocyanatocorrole derivatives (1–6). Besides that, while treating the reaction mixture with another radical inhibitor, like BHT {BHT = butylated hydroxytoluene}, we have observed the formation of an adduct of BHT with a thiocyanate radical. The adduct was characterized by ESI-MS spectra (Figure S3). While performing the reaction of 5,10,15-tris(4-cyanophenyl)corrole with NH_4SCN under irradiation with a CFL lamp, we have observed the presence of $(\text{SCN})_2$ in the reaction mixture by ESI-MS spectra (Figure S4). The origin of $(\text{SCN})_2$ can be demonstrated via the coupling of two thiocyanate radicals. All this evidence supports the formation of a thiocyanate radical via the photoexcitation of a mixture of free base corrole and NH_4SCN . It has been observed that the excited state of porphyrinoids is more potent oxidants and reductants in comparison to their ground state. The oxidation and reduction potential in the excited state of corroles can be estimated from the Gibbs energy of the PET {PET = photoinduced electron transfer} processes.⁵⁸ For example, the reduction potential of the 5,10,15-tris(4-cyanophenyl)corrole in the excited state was found out to be +1.03 V vs SCE (see the Supporting Information for Mechanistic Studies, Figures S5–S7). This value is higher than the oxidation potential of NH_4SCN ($E_{\text{ox}} = 0.65$ V vs SCE). Thus, the oxidation of NH_4SCN is thermodynamically favorable. In addition to that, we have also recorded the EPR spectrum of a mixture of 5,10,15-tris(4-cyanophenyl)corrole and NH_4SCN in CH_3CN solution under the irradiation of a CFL lamp (20 W) at 298 K. An isotropic EPR signal is observed with a *g* value of 2.003 (Figure 6). A peak-to-peak separation of 15 G is also observed. However, the hyperfine coupling due to nitrogen nuclei is not resolved. The isotropic EPR signal having a narrow line width and a *g* value close to the free radical value indicates a corrole based radical.⁵⁹

This, in conjunction with the favorable reduction potential of the FB corrole, clearly indicates the generation of a corrole based radical anion (corrole $^{\bullet-}$). On the basis of the above

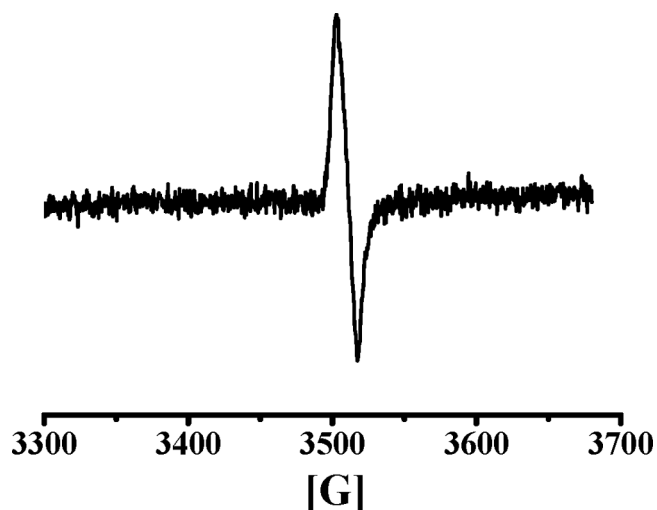
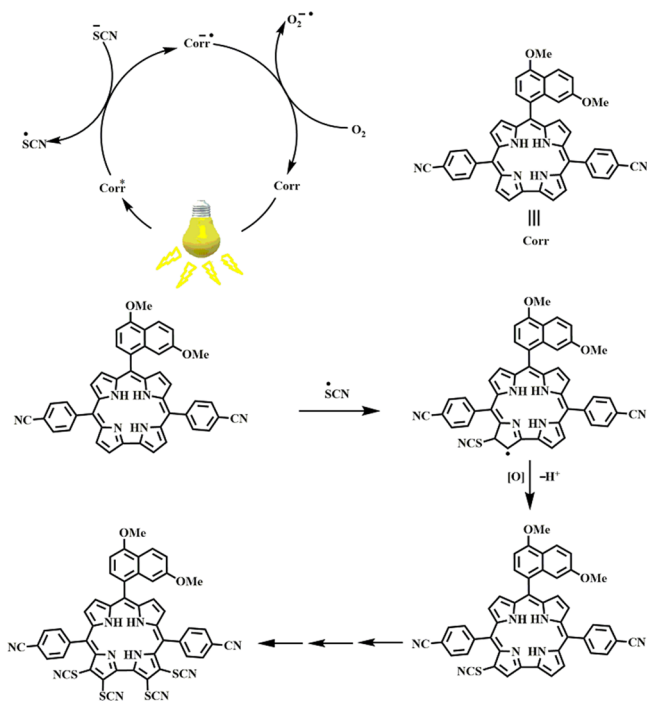


Figure 6. EPR spectrum of a mixture of 5,10,15-tris(4-cyanophenyl)corrole and NH_4SCN in CH_3CN solution under the irradiation of a CFL lamp (20 W) at 298 K.

observations, and also from the previous literatures,³⁹ we have proposed a plausible mechanism for the formation of tetrathiocyanatocorrole derivatives (1–6) (Scheme 3). FB

Scheme 3. Proposed Mechanism



corroles and NH_4SCN in CH_3CN solution under the irradiation of a CFL lamp resulted in the formation of excited corroles (corrole*). In the next step, a single electron is transferred from SCN^- anion to the excited corroles (corrole*), and this resulted in the generation of a $\bullet\text{SCN}$ radical and corrole radical anion (corrole \bullet^-), respectively.

This corrole radical anion can be quenched via the transfer of an extra electron to atmospheric O_2 , and it thus resulted in the formation of $\text{O}_2\bullet^-$. In the succeeding step, the generated $\bullet\text{SCN}$ radical can directly couple with the corrole macrocycle and produce the monothiocyanatocorrole radical intermediate.

Subsequent oxidation, followed by deprotonation, resulted in the formation of monothiocyanatocorrole derivatives. The process can work cyclically and generates the tetrathiocyanatocorrole derivatives (1–6). We have used the NH_4SCN in excess quantities, which thus is responsible for the insertion of four thiocyanato groups in the corrole periphery.

CONCLUSIONS

In conclusion, we have developed a new synthetic methodology for the facile synthesis of a new class of corrole ligands bearing four thiocyanate groups at the four neighboring β -positions (2, 3, 17, and 18) in the corrole periphery. To date, there is no synthetic protocol available in the literature that describes the synthesis of tetrathiocyanatocorroles in general. A photocatalytic synthetic pathway was developed for the first time to establish the synthesis of these new classes of tetra-substituted corroles (1–6). Single-crystal XRD analysis reveals that these tetrathiocyanatocorrole macrocycles (1–6) are significantly distorted and exist as $\alpha_2\beta_2$ atropisomers. The mechanism of this reaction has been thoroughly investigated, and it indicates that a radical pathway is involved. The absorption and emission spectra of these tetrathiocyanatocorrole macrocycles (1–6) vary significantly in comparison to those of the starting free base corroles (1A–6A). In the absorption spectra, the Soret region is split into three bands of equal intensity and the intensity of the Q bands is significantly strengthened. This can be considered as a rare occasion in which the intensity of Soret and Q bands equalizes. The absorption feature of these modified corrole derivatives (both position and intensity) bears a nice similarity with the naturally occurring chromophore, chlorophyll-*a*. Thus, these newly synthesized molecules can be considered as a spectroscopic model for chlorophyll-*a* pigments. The emission region is significantly red-shifted and falls in the NIR region. In a representative corrolato Au(III) complex (2-Au), the observed Au \cdots H–C interactions certainly point out that these Au(III)-corrole complexes are capable of activating the unfunctionalized C–H groups via weak interactions and thus will have potential implications in C–H activation reactions.⁶⁰ Thus, the present synthetic protocol will pave the way for the future development of a new series of FB corroles and their possible metal complexes for a wide range of applications.

EXPERIMENTAL SECTION

Materials. The precursor's pyrrole, *p*-chloranil, and aldehydes were purchased from Aldrich, USA. NH_4SCN (>98.5% purity) and acetonitrile (HPLC) were purchased from Merck Pvt. Ltd Chemicals. Other chemicals were of reagent grade. Hexane, CH_2Cl_2 , and CH_3CN were distilled from KOH and CaH_2 , respectively. For spectroscopy studies, HPLC grade solvents were used. For the synthesis of FB corroles, a protocol developed by Gryko et al. was used. The synthetic methodologies and full spectroscopic characterization of free base corroles, 5,10,15-triphenylcorrole, 5,10,15-tris(4-cyanophenyl)corrole, 5,10,15-tris(4-nitrophenyl)corrole, 5,10,15-tris(pentafluorophenyl)corrole, 10-(4-bromophenyl)-5,15-bis(4-cyanophenyl)corrole, and 10-(4,7-dimethoxynaphthalen-1-yl)-5,15-bis(4-cyanophenyl)corrole, are provided in the previous literatures.^{27,32,33}

Physical Measurements. The elemental analyses were carried out with a Euro EA elemental analyzer. UV–vis spectral studies were performed on a Perkin-Elmer LAMBDA-750 spectrophotometer. Emission spectral studies were performed on a Shimadzu RF-6000 spectrofluorophotometer using an optical cell of 1 cm path length. FT-IR spectra were recorded on a Perkin-Elmer spectrophotometer with samples prepared as KBr pellets. The NMR measurements were carried out using a Bruker 400 MHz NMR spectrometer. Chemical

shifts are expressed in parts per million (ppm) relative to residual acetonitrile ($\delta = 1.93$). Electro spray mass spectra were recorded on a Bruker Micro TOF-QII mass spectrometer. Cyclic voltammetry measurements were carried out using a CS350 electrochemical test system (China). A glassy carbon working electrode, a platinum wire as an auxiliary electrode, and a Ag-AgCl reference electrode were used in a three-electrode configuration. Tetrabutylammonium perchlorate (TBAP) was the supporting electrolyte (0.1 M), and the concentration of the solution was 10^{-3} M with respect to the complex. The half-wave potential E_{298}^0 was set equal to 0.5 ($E_{pa} + E_{pc}$), where E_{pa} and E_{pc} are anodic and cathodic cyclic voltammetric peak potentials, respectively. The scan rate used was 100 mV s^{-1} . EPR spectra at X-band frequency (ca. 9.5 GHz) were obtained with a Bruker EMX (ER 073) System. The measurements were carried out in synthetic quartz glass tubes. For light promoted reactions, a Philips energy saver CFL/LED lamp 20W B22 (200–240 V, ~50 Hz; Luminous Flux: 2000 lm; Photometric Code: 865/15157; crystal white/6500k) was placed in front of the borosilicate reaction vessel at a distance of 20 cm without any filter.

Crystal Structure Determination. See the Supporting Information.

Synthesis of 2,3,17,18-Tetrathiocyanato-5,10,15-triphenylcorrole, 1. 50 mg (0.095 mmol) of 5,10,15-triphenylcorrole was dissolved in 15 mL of acetonitrile, and then 500 mg of NH_4SCN (6.6 mmol) was added to it. The reaction mixture was stirred at room temperature under irradiation with a CFL/LED lamp (20 W) for 2.5 h in the air. At this point, the second batch of reagents, NH_4SCN (500 mg) and acetonitrile (15 mL) were added to the reaction mixture. The solution was stirred for another 2.5 h. The residual solvent was evaporated to dryness, and the crude product was dissolved in dichloromethane. The crude product was purified by using column chromatography through silica gel (100–200 mesh). The desired product was eluted by using a mixture of 97% DCM and 3% acetonitrile. The final form of the compound was obtained as green crystalline materials.

For 2,3,17,18-Tetrathiocyanato-5,10,15-triphenylcorrole, 1. Yield: 30% (21 mg). Anal. Calcd for $\text{C}_{41}\text{H}_{22}\text{N}_8\text{S}_4$ (1): C, 65.23; H, 2.94; N, 14.84. Found: C, 65.34; H, 2.99; N, 14.71. $\lambda_{\text{max}}/\text{nm}$ ($\epsilon/\text{M}^{-1}\text{cm}^{-1}$) in CH_2Cl_2 : 408 (32000), 433 (30000), 456 (34000), 539 (7000), 581 (15700), 632 (14000), 686 (34000) (Figure S8). ^1H NMR (400 MHz, Chloroform-*d*) δ 8.17 (m, 2H), 7.96 (m, 4H), 7.86 (m, 4H), 7.72 (m, 6H), 7.64 (m, 3H). 1 displayed strong fluorescence at 734 nm in CH_2Cl_2 (Figure S15). HRMS (ESI) m/z : [$1 - \text{H}$] $^-$ Calcd for $\text{C}_{41}\text{H}_{21}\text{N}_8\text{S}_4$ 753.0767; Found 753.1355 (Figure S27).

Synthesis of 2,3,17,18-Tetrathiocyanato-5,10,15-tris(4-cyanophenyl)corrole, 2. 50 mg (0.083 mmol) of 5,10,15-tris(4-cyanophenyl)corrole was dissolved in 15 mL of acetonitrile, and then 500 mg of NH_4SCN (6.6 mmol) was added to it. The reaction mixture was stirred at room temperature under irradiation with a CFL/LED lamp (20 W) for 2.5 h in the air. At this point, the second batch of reagents, NH_4SCN (500 mg) and acetonitrile (15 mL) were added to the reaction mixture. The solution was stirred for another 2.5 h. The residual solvent was evaporated to dryness, and the crude product was dissolved in dichloromethane. The crude product was purified by using column chromatography through silica gel (100–200 mesh). The desired product was eluted by using a mixture of 85% DCM and 15% acetonitrile. The final form of the compound was obtained as green crystalline materials.

For 2,3,17,18-Tetrathiocyanato-5,10,15-tris(4-cyanophenyl)corrole, 2. Yield: 32% (22 mg). Anal. Calcd for $\text{C}_{44}\text{H}_{19}\text{N}_{11}\text{S}_4$ (2): C, 63.67; H, 2.31; N, 18.56. Found: C, 63.54; H, 2.20; N, 18.43. $\lambda_{\text{max}}/\text{nm}$ ($\epsilon/\text{M}^{-1}\text{cm}^{-1}$) in CH_3CN : 400 (41671), 426 (38104), 451 (37821), 528 (9656), 570 (17030), 619 (20716), 671 (37985) (Figure S9). ^1H NMR (400 MHz, Acetonitrile-*d*₃) δ 8.09 (d, $J = 7.8$ Hz, 4H), 8.03 (d, $J = 7.9$ Hz, 4H), 7.99 (d, $J = 3.5$ Hz, 4H), 7.95 (d, $J = 4.8$ Hz, 2H), 7.74 (d, $J = 5.0$ Hz, 2H). ^{13}C { ^1H } NMR (101 MHz, CD_3CN) δ 150.7, 145.7, 143.8, 137.5, 136.1, 133.8, 131.2, 129.8, 128.3, 125.6, 123.5, 122.2, 119.1, 117.3, 113.7, 111.8, 111.3, 110.6. 2 displayed strong fluorescence at 712 nm in CH_3CN (Figure S16).

HRMS (ESI) m/z : [$2 - \text{H}$] $^-$ Calcd for $\text{C}_{44}\text{H}_{18}\text{N}_{11}\text{S}_4$ 828.0624; Found 828.1856 (Figure S28).

Synthesis of 2,3,17,18-Tetrathiocyanato-5,10,15-tris(4-nitrophenyl)corrole, 3. 50 mg (0.076 mmol) of 5,10,15-tris(4-nitrophenyl)corrole was dissolved in 15 mL of acetonitrile, and then 500 mg of NH_4SCN (6.6 mmol) was added to it. The reaction mixture was stirred at room temperature under irradiation with a CFL/LED lamp (20 W) for 2.5 h in the air. At this point, the second batch of reagents, NH_4SCN (500 mg) and acetonitrile (15 mL) were added to the reaction mixture. The solution was stirred for another 2.5 h. The residual solvent was evaporated to dryness, and the crude product was dissolved in dichloromethane. The crude product was purified by using column chromatography through silica gel (100–200 mesh). The desired product was eluted by using a mixture of 85% DCM and 15% acetonitrile. The final form of the compound was obtained as green crystalline materials.

For 2,3,17,18-Tetrathiocyanato-5,10,15-tris(4-nitrophenyl)corrole, 3. Yield: 12% (8 mg). Anal. Calcd for $\text{C}_{41}\text{H}_{19}\text{N}_{11}\text{O}_6\text{S}_4$ (3): C, 55.34; H, 2.15; N, 17.31. Found: C, 55.45; H, 2.23; N, 17.24. $\lambda_{\text{max}}/\text{nm}$ ($\epsilon/\text{M}^{-1}\text{cm}^{-1}$) in CH_3CN : 403 (35000), 430 (35200), 457 (38600), 532 (10400), 573 (13500), 621 (18000), 674 (41000) (Figure S10). ^1H NMR (400 MHz, Acetonitrile-*d*₃) δ 8.41–8.27 (m, 6H), 7.96 (d, $J = 13.0$ Hz, 6H), 7.84 (s, 2H), 7.68 (m, 2H). ^{13}C { ^1H } NMR (101 MHz, CD_3CN) δ 151.1, 148.8, 146.4, 143.3, 140.3, 136.9, 135.5, 133.2, 131.9, 129.3, 123.3, 112.8, 112.1, 109.1, 107.1, 105.7. HRMS (ESI) m/z : [$3 - \text{H}$] $^-$ Calcd for $\text{C}_{41}\text{H}_{18}\text{N}_{11}\text{O}_6\text{S}_4$ 888.0319; Found 888.2065 (Figure S29).

Synthesis of 2,3,17,18-Tetrathiocyanato-5,10,15-tris(pentafluorophenyl)corrole, 4. 50 mg (0.063 mmol) of 5,10,15-tris(pentafluorophenyl)corrole was dissolved in 15 mL of acetonitrile, and then 500 mg of NH_4SCN (6.6 mmol) was added to it. The reaction mixture was stirred at room temperature under irradiation with a CFL/LED lamp (20 W) for 2.5 h in the air. At this point, the second batch of reagents, NH_4SCN (500 mg) and acetonitrile (15 mL) were added to the reaction mixture. The solution was stirred for another 2.5 h. The residual solvent was evaporated to dryness, and the crude product was dissolved in dichloromethane. The crude product was purified by using column chromatography through silica gel (100–200 mesh). The desired product was eluted by using a mixture of 88% DCM and 12% acetonitrile. The final form of the compound was obtained as sea green crystalline materials.

For 2,3,17,18-Tetrathiocyanato-5,10,15-tris(pentafluorophenyl)corrole, 4. Yield: 35% (22 mg). Anal. Calcd for $\text{C}_{41}\text{H}_7\text{F}_{15}\text{N}_8\text{S}_4$ (4): C, 48.05; H, 0.69; N, 10.93. Found: C, 48.13; H, 0.77; N, 10.86. $\lambda_{\text{max}}/\text{nm}$ ($\epsilon/\text{M}^{-1}\text{cm}^{-1}$) in CH_3CN : 407 (65000), 441 (55000), 528 (10300), 577 (28000), 601 (28500), 651 (60500) (Figure S11). ^1H NMR (400 MHz, Chloroform-*d*) δ 7.93 (d, $J = 4.9$ Hz, 2H), 7.66 (d, $J = 4.8$ Hz, 2H). ^{19}F { ^1H } NMR (377 MHz, Chloroform-*d*) δ -137.3 (m, 6F), -152.8 (m, 3F), -161.9 (m, 6F). 4 displayed strong fluorescence at 677 nm in CH_3CN (Figure S17). HRMS (ESI) m/z : [$4 - \text{H}$] $^-$ Calcd for $\text{C}_{41}\text{H}_6\text{F}_{15}\text{N}_8\text{S}_4$ 1022.9353; Found 1022.9972 (Figure S30).

Synthesis of 2,3,17,18-Tetrathiocyanato-10-(4-bromophenyl)-5,15-bis(4-cyanophenyl)corrole, 5. 50 mg (0.076 mmol) of 10-(4-bromophenyl)-5,15-bis(4-cyanophenyl)corrole was dissolved in 15 mL of acetonitrile, and then 500 mg of NH_4SCN (6.6 mmol) was added to it. The reaction mixture was stirred at room temperature under irradiation with a CFL/LED lamp (20 W) for 2.5 h in the air. At this point, the second batch of reagents, NH_4SCN (500 mg) and acetonitrile (15 mL) were added to the reaction mixture. The solution was stirred for another 2.5 h. The residual solvent was evaporated to dryness, and the crude product was dissolved in dichloromethane. The crude product was purified by using column chromatography through silica gel (100–200 mesh). The desired product was eluted by using a mixture of 90% DCM and 10% acetonitrile. The final form of the compound was obtained as green crystalline materials.

For 2,3,17,18-Tetrathiocyanato-10-(4-bromophenyl)-5,15-bis(4-cyanophenyl)corrole, 5. Yield: 48% (32 mg). Anal. Calcd for $\text{C}_{43}\text{H}_{19}\text{N}_{10}\text{S}_4\text{Br}$ (5): C, 58.43; H, 2.17; N, 15.85. Found: C, 58.57; H, 2.28; N, 15.71. $\lambda_{\text{max}}/\text{nm}$ ($\epsilon/\text{M}^{-1}\text{cm}^{-1}$) in CH_3CN : 399 (38567), 423 (33328), 450 (29059), 530 (11358), 568 (16597), 619 (18791), 673

(28850) (Figure S12). ^1H NMR (400 MHz, Acetonitrile- d_3) δ 7.97 (m, 8H), 7.84 (d, $J = 4.7$ Hz, 2H), 7.69 (m, 6H). ^{13}C $\{^1\text{H}\}$ NMR (101 MHz, CD_3CN) δ 163.4, 152.0, 146.8, 144.9, 141.4, 137.1, 136.3, 134.7, 133.1, 132.1, 131.6, 131.2, 129.6, 122.0, 120.0, 117.2, 112.7, 112.3, 111.1, 109.2, 106.5. **5** displayed strong fluorescence at 722 nm in acetonitrile (Figure S18). HRMS (ESI) m/z : $[\text{5} + \text{H}]^+$ Calcd for $\text{C}_{43}\text{H}_{20}\text{N}_{10}\text{S}_4\text{Br}$ 882.9758; Found 883.2458 (Figure S31).

Synthesis of 2,3,17,18-Tetrathiocyanato-10-(4,7-dimethoxynaphthalen-1-yl)-5,15-bis(4-cyanophenyl)corrole, 6. 50 mg (0.073 mmol) of 10-(4,7-dimethoxynaphthalen-1-yl)-5,15-bis(4-cyanophenyl)corrole was dissolved in 15 mL of acetonitrile, and then 500 mg of NH_4SCN (6.6 mmol) was added to it. The reaction mixture was stirred at room temperature under irradiation with a CFL/LED lamp (20 W) for 2.5 h in the air. At this point, the second batch of reagents, NH_4SCN (500 mg) and acetonitrile (15 mL) were added to the reaction mixture. The solution was stirred for another 2.5 h. The residual solvent was evaporated to dryness, and the crude product was dissolved in dichloromethane. The crude product was purified by using column chromatography through silica gel (100–200 mesh). The desired product was eluted by using a mixture of 80% DCM and 20% acetonitrile. The final form of the compound was obtained as green crystalline materials.

For 2,3,17,18-Tetrathiocyanato-10-(4,7-dimethoxynaphthalen-1-yl)-5,15-bis(4-cyanophenyl)corrole, **6**. Yield: 45% (30 mg). Anal. Calcd for $\text{C}_{49}\text{H}_{26}\text{N}_{10}\text{O}_2\text{S}_4$ (**6**): C, 64.32; H, 2.86; N, 15.31. Found: C, 64.23; H, 2.73; N, 15.44. $\lambda_{\text{max}}/\text{nm}$ ($\epsilon/\text{M}^{-1}\text{cm}^{-1}$) in CH_3CN : 399 (38537), 422 (33403), 449 (28940), 529 (11477), 569 (16716), 621 (18764), 673 (28806) (Figure S13). ^1H NMR (400 MHz, Acetonitrile- d_3) δ 8.27 (d, $J = 9.4$ Hz, 1H), 8.04–7.84 (m, 8H), 7.68 (m, 3H), 7.41 (s, 2H), 7.06 (d, $J = 9.7$ Hz, 1H), 6.89 (d, $J = 7.9$ Hz, 1H), 6.52 (s, 1H), 4.05 (s, 3H), 3.09 (s, 3H). ^{13}C $\{^1\text{H}\}$ NMR (101 MHz, CD_3CN) δ 159.1, 156.5, 134.8, 134.6, 133.5, 132.1, 131.5, 130.7, 129.9, 129.7, 129.6, 124.6, 121.1, 120.0, 117.6, 112.8, 112.3, 112.1, 107.4, 106.5, 105.2, 102.3, 56.3, 55.3. **6** displayed strong fluorescence at 733 nm in acetonitrile (Figure S19). HRMS (ESI) m/z : $[\text{6} - \text{H}]^-$ Calcd for $\text{C}_{49}\text{H}_{25}\text{N}_{10}\text{O}_2\text{S}_4$ 913.1039; Found 913.4438 (Figure S32).

Synthesis of {2,3,17,18-Tetrathiocyanato-5,10,15-tris(4-cyanophenyl) Corrolato-Au(III)}, 2-Au. For the insertion of Au(III) in the corrole cavity, a previously reported protocol was followed.⁵⁰ 32 mg (0.04 mmol) of 2,3,17,18-tetrathiocyanato-5,10,15-tris(4-cyanophenyl)corrole was dissolved in 10 mL of acetonitrile, and then the excess of gold acetate (112 mg; 0.30 mmol) was added to it, followed by pyridine (10 mL). The reaction mixture was stirred for 45 min under room temperature. After that, the solvent was evaporated and the brown color crude product was subjected to column chromatography using a silica gel (100–200 mesh) column. The desired product (reddish blue) was eluted by using a mixture of 96% DCM and 4% acetonitrile. The final form of the compound was obtained as reddish-pink crystalline materials.

For {2,3,17,18-Tetrathiocyanato-5,10,15-tris(4-cyanophenyl) Corrolato-Au(III)}, 2-Au. Yield: 46% (18 mg). Anal. Calcd for $\text{C}_{44}\text{H}_{16}\text{AuN}_{11}\text{S}_4$ (**2-Au**): C, 51.61; H, 1.58; N, 15.05. Found: C, 51.74; H, 1.69; N, 14.97. $\lambda_{\text{max}}/\text{nm}$ ($\epsilon/\text{M}^{-1}\text{cm}^{-1}$) in CH_2Cl_2 : 404 (62628), 422 (60304), 536 (16883), 551 (21900), 577 (54309), 593 (64535) (Figure S14). ^1H NMR (400 MHz, CDCl_3) δ 8.50–8.42 (m, 4H), 8.23–8.06 (m, 12H). ^{13}C $\{^1\text{H}\}$ NMR (101 MHz, CDCl_3) δ 171.9, 153.2, 150.3, 147.3, 144.4, 142.8, 140.9, 133.6, 131.8, 128.2, 120.5, 118.0, 115.5, 114.3, 113.2, 109.6. HRMS (ESI) m/z : $[\text{2-Au} + \text{Na}]^+$ Calcd for $\text{C}_{44}\text{H}_{16}\text{AuN}_{11}\text{S}_4\text{Na}$ 1046.0036; Found 1046.0104 (Figure S33).

■ ASSOCIATED CONTENT

Supporting Information

The Supporting Information is available free of charge at <https://pubs.acs.org/doi/10.1021/acs.joc.0c02683>.

Mechanistic studies, crystallographic data, UV–vis, FT-IR, ESI-MS, ^1H NMR, and ^{13}C NMR data (PDF)

Accession Codes

CCDC 2043450 and 2043451 contain the supplementary crystallographic data for this paper. These data can be obtained free of charge via www.ccdc.cam.ac.uk/data_request/cif, or by emailing data_request@ccdc.cam.ac.uk, or by contacting The Cambridge Crystallographic Data Centre, 12 Union Road, Cambridge CB2 1EZ, UK; fax: +44 1223 336033.

■ AUTHOR INFORMATION

Corresponding Author

Sanjib Kar – School of Chemical Sciences, National Institute of Science Education and Research (NISER), Bhubaneswar 752050, India; Homi Bhabha National Institute, Mumbai 400 094, India; orcid.org/0000-0002-0203-8884; Email: sanjib@niser.ac.in

Authors

Kasturi Sahu – School of Chemical Sciences, National Institute of Science Education and Research (NISER), Bhubaneswar 752050, India; Homi Bhabha National Institute, Mumbai 400 094, India

Sruti Mondal – School of Chemical Sciences, National Institute of Science Education and Research (NISER), Bhubaneswar 752050, India; Homi Bhabha National Institute, Mumbai 400 094, India

Shaikh M. Mobin – Disciplines of Metallurgical Engineering and Materials Science (MEMS) and Bioscience and Biomedical Engineering (BSBE), Indian Institute of Technology Indore, Indore 453552, India; orcid.org/0000-0003-1940-3822

Complete contact information is available at: <https://pubs.acs.org/10.1021/acs.joc.0c02683>

Notes

The authors declare no competing financial interest.

■ ACKNOWLEDGMENTS

Financial support received from the Department of Atomic Energy (India) is gratefully acknowledged. The authors thankfully acknowledge NISER-Bhubaneswar for providing the infrastructure. The authors gratefully acknowledge the financial support provided by SERB (Science & Engineering Research Board), India (EMR/2016/005484), to carry out this research work. K.S. thanks CSIR India for the research fellowship.

■ DEDICATION

Dedicated to Professor Wolfgang Kaim on the occasion of his 70th birthday.

■ REFERENCES

- Bonnett, R.; Berenbaum, M. *Porphyryns as photosensitizers. In Photosensitizing compounds: Their chemistry, biology and clinical use*; Wiley, 1989; pp 40–59.
- Handbook Of Photodynamic Therapy: Updates On Recent Applications Of Porphyrin-based Compounds*; David, K., Ed.; World Scientific, 2016.
- Pereira, P. M.; Tomé, J. P.; Fernandes, R. *Molecular Targeted Photodynamic Therapy for Cancer. In Towards Diagnostics and Treatment of Cancer; Handbook of Porphyrin Science: With Applications to Chemistry, Physics, Materials Science, Engineering, Biology and Medicine, Vol. 39*; World Scientific, 2016; pp 127–169.

- (4) Rybicka-Jasińska, K.; Shan, W.; Zawada, K.; Kadish, K. M.; Gryko, D. Porphyrins as photoredox catalysts: Experimental and theoretical studies. *J. Am. Chem. Soc.* **2016**, *138*, 15451–15458.
- (5) Rybicka-Jasińska, K.; Koenig, B.; Gryko, D. Porphyrin-Catalyzed Photochemical C–H Arylation of Heteroarenes. *Eur. J. Org. Chem.* **2017**, *2017*, 2104–2107.
- (6) Costa e Silva, R.; Oliveira da Silva, L.; de Andrade Bartolomeu, A.; Brocksom, T. J.; de Oliveira, K. T. Recent applications of porphyrins as photocatalysts in organic synthesis: batch and continuous flow approaches. *Beilstein J. Org. Chem.* **2020**, *16*, 917–955.
- (7) Prier, C. K.; Rankic, D. A.; MacMillan, D. W. C. Visible light photoredox catalysis with transition metal complexes: applications in organic synthesis. *Chem. Rev.* **2013**, *113*, 5322–5363.
- (8) Zeitler, K. *Metal-free Photo (redox) Catalysis*; Wiley-VCH: Weinheim, 2018.
- (9) Guillard, R.; Kadish, K. M.; Smith, K. M.; Guillard, R. *The porphyrin handbook*; Academic Press: New York, 2003.
- (10) Patra, B.; Mondal, S.; Kar, S. Corroles. In *Encyclopedia of Inorganic and Bioinorganic Chemistry*; Scott, R. A., Storr, T., Eds.; John Wiley & Sons, Ltd.: Chichester, U.K., 2020. DOI: 10.1002/9781119951438.eibc2729.
- (11) Paolesse, R.; Nardis, S.; Stefanelli, M.; Fronczek, F. R.; Vicente, M. G. H. Hemiporphycene from the Expansion of a Corrole Ring. *Angew. Chem., Int. Ed.* **2005**, *44*, 3047–3050.
- (12) Dogutan, D. K.; McGuire Jr, R.; Nocera, D. G. Electrocatalytic water oxidation by cobalt (III) hangman β -octafluoro corroles. *J. Am. Chem. Soc.* **2011**, *133*, 9178–9180.
- (13) Autret, M.; Will, S.; Caemelbecke, E. V.; Lex, J.; Gisselbrecht, J.-P.; Gross, M.; Vogel, E.; Kadish, K. M. Synthesis and Electrochemistry of Iron (III) Corroles Containing a Nitrosyl Axial Ligand. Spectral Characterization of [(OEC) Fe(III) (NO)]_n where n = 0, 1, 2, or-1 and OEC is the Trianion of 2, 3, 7, 8, 12, 13, 17, 18-Octaethylcorrole. *J. Am. Chem. Soc.* **1994**, *116*, 9141–9149.
- (14) Liu, H.-Y.; Yam, F.; Xie, Y.-T.; Li, X.-Y.; Chang, C. K. A Bulky Bis-Pocket Manganese (V)-Oxo Corrole Complex: Observation of Oxygen Atom Transfer between Triply Bonded Mn^V=O and Alkene. *J. Am. Chem. Soc.* **2009**, *131*, 12890–12891.
- (15) Brizet, B.; Desbois, N.; Bonnot, A.; Langlois, A.; Dubois, A.; Barbe, J.-M.; Gros, C. P.; Goze, C.; Denat, F.; Harvey, P. D. Slow and fast singlet energy transfers in BODIPY-gallium (III) corrole dyads linked by flexible chains. *Inorg. Chem.* **2014**, *53*, 3392–3403.
- (16) Aviv, I.; Gross, Z. Corrole-based applications. *Chem. Commun.* **2007**, 1987–1999.
- (17) Thomas, K. E.; Vazquez-Lima, H.; Fang, Y.; Song, Y.; Gagnon, K. J.; Beavers, C. M.; Kadish, K. M.; Ghosh, A. Ligand Noninnocence in Coinage Metal Corroles: A Silver Knife-Edge. *Chem. - Eur. J.* **2015**, *21*, 16839–16847.
- (18) Mondal, S.; Naik, P. K.; Adha, J. K.; Kar, S. Synthesis, characterization, and reactivities of high valent metal–corrole (M = Cr, Mn, and Fe) complexes. *Coord. Chem. Rev.* **2019**, *400*, 213043.
- (19) Nardis, S.; Mandoj, F.; Stefanelli, M.; Paolesse, R. Metal complexes of corrole. *Coord. Chem. Rev.* **2019**, *388*, 360–405.
- (20) Aviv-Harel, I.; Gross, Z. Aura of corroles. *Chem. - Eur. J.* **2009**, *15*, 8382–8394.
- (21) Ghosh, A. Electronic structure of corrole derivatives: Insights from molecular structures, spectroscopy, electrochemistry, and quantum chemical calculations. *Chem. Rev.* **2017**, *117*, 3798–3881.
- (22) Orłowski, R.; Gryko, D.; Gryko, D. T. Synthesis of corroles and their heteroanalogues. *Chem. Rev.* **2017**, *117*, 3102–3137.
- (23) Fang, Y.; Ou, Z.; Kadish, K. M. Electrochemistry of corroles in nonaqueous media. *Chem. Rev.* **2017**, *117*, 3377–3419.
- (24) Fujino, K.; Hirata, Y.; Kawabe, Y.; Morimoto, T.; Srinivasan, A.; Toganoh, M.; Miseki, Y.; Kudo, A.; Furuta, H. Confusion and Neo-Confusion: Corrole Isomers with an NNNC Core. *Angew. Chem., Int. Ed.* **2011**, *50*, 6855–6859.
- (25) Hiroto, S.; Furukawa, K.; Shinokubo, H.; Osuka, A. Synthesis and biradicaloid character of doubly linked corrole dimers. *J. Am. Chem. Soc.* **2006**, *128*, 12380–12381.
- (26) Sinha, W.; Sommer, M. G.; Deibel, N.; Ehret, F.; Bauer, M.; Sarkar, B.; Kar, S. Experimental and theoretical investigations of the existence of Cu^{II}, Cu^{III}, and Cu^{IV} in copper corrolato complexes. *Angew. Chem., Int. Ed.* **2015**, *54*, 13769–13774.
- (27) Sinha, W.; Sommer, M. G.; Deibel, N.; Ehret, F.; Sarkar, B.; Kar, S. Silver Corrole Complexes: Unusual Oxidation States and Near-IR-Absorbing Dyes. *Chem. - Eur. J.* **2014**, *20*, 15920–15932.
- (28) Sinha, W.; Sommer, M. G.; Van der Meer, M.; Plebst, S.; Sarkar, B.; Kar, S. Structural, electrochemical and spectroelectrochemical study on the geometric and electronic structures of [(corrolato)Au^{III}]ⁿ (n = 0, +1, -1) complexes. *Dalton Trans.* **2016**, *45*, 2914–2923.
- (29) Patra, B.; Sobottka, S.; Sinha, W.; Sarkar, B.; Kar, S. Isovalent Ag^{III}/Ag^{III}, Ag^{II}/Ag^{II}, Mixed-Valent Ag^{II}/Ag^{III}, and Corrolato-Based Mixed-Valency in β , β' -Linked [Bis {corrolato-silver}]ⁿ Complexes. *Chem. - Eur. J.* **2017**, *23*, 13858–13863.
- (30) Sinha, W.; Sommer, M. G.; Hettmanczyk, L.; Patra, B.; Filippou, V.; Sarkar, B.; Kar, S. Ruthenium–Ruthenium-Bonded [Bis {corrolato-ruthenium (III)}]ⁿ (n = 0, +1, -1) Complexes: Model Compounds for the Photosynthetic Special Pair. *Chem. - Eur. J.* **2017**, *23*, 2396–2404.
- (31) Patra, B.; Sobottka, S.; Mondal, S.; Sarkar, B.; Kar, S. Metal coordination induced ring contraction of porphyrin derivatives. *Chem. Commun.* **2018**, *54*, 9945–9948.
- (32) Kozarna, B.; Gryko, D. T. Efficient synthesis of meso-substituted corroles in a H₂O-MeOH mixture. *J. Org. Chem.* **2006**, *71*, 3707–3717.
- (33) Gross, Z.; Galili, N.; Simkhovich, L.; Saltsman, I.; Botoshansky, M.; Blaser, D.; Boese, R.; Goldberg, I. Solvent-free condensation of pyrrole and pentafluorobenzaldehyde: A novel synthetic pathway to corrole and oligopyrromethenes. *Org. Lett.* **1999**, *1*, 599–602.
- (34) Mahammed, A.; Gross, Z. Corroles as triplet photosensitizers. *Coord. Chem. Rev.* **2019**, *379*, 121–132.
- (35) Lemon, C. M. Corrole photochemistry. *Pure Appl. Chem.* **2020**, *92*, 1901–1919.
- (36) Guy, R. G. In *The Chemistry of Cyanates and Their Thio Derivatives*; Patai, S., Ed.; John Wiley & Sons: New York, 1977; Part 2, p 819.
- (37) Hill, H. A. O. In *Chemistry and Biochemistry of Thiocyanic Acid and Its Derivatives*; Newman, A. A., Ed.; Academic Press: London, 1975.
- (38) Fan, W.; Yang, Q.; Xu, F.; Li, P. A visible-light-promoted aerobic metal-free C-3 thiocyanation of indoles. *J. Org. Chem.* **2014**, *79*, 10588–10592.
- (39) Mitra, S.; Ghosh, M.; Mishra, S.; Hajra, A. Metal-free thiocyanation of imidazoheterocycles through visible light photoredox catalysis. *J. Org. Chem.* **2015**, *80*, 8275–8281.
- (40) Nikoofar, K. A brief on thiocyanation of N-activated arenes and N-bearing heteroaromatic compounds. *Chem. Sci. Trans.* **2013**, *2*, 691–700.
- (41) Barata, J. F.; Neves, M. G. P.; Faustino, M. A. F.; Tomé, A. C.; Cavaleiro, J. A. Strategies for corrole functionalization. *Chem. Rev.* **2017**, *117*, 3192–3253.
- (42) Barata, J. F. B.; Santos, C. I. M.; Neves, M. G. P. M. S.; Faustino, M. A. F.; Cavaleiro, J. A. S. Functionalization of Corroles. In *Synthesis and Modifications of Porphyrinoids*; Paolesse, R., Ed.; Topics in Heterocyclic Chemistry, Vol. 33; Springer-Verlag: Berlin, 2014; pp 79–141.
- (43) Lemon, C. M.; Brothers, P. J. The Synthesis, Reactivity, and Peripheral Functionalization of Corroles. *J. Porphyrins Phthalocyanines* **2011**, *15*, 809–834.
- (44) Nardis, S.; Pomarico, G.; Stefanelli, M.; Lentini, S.; Cicero, D. O.; Fronczek, F. R.; Smith, K. M.; Paolesse, R. The Scope of the β -Halogenation of Triarylcorroles. *J. Porphyrins Phthalocyanines* **2016**, *20*, 465–474.
- (45) Lemon, C. M.; Halbach, R. L.; Huynh, M.; Nocera, D. G. Photophysical properties of β -substituted free-base corroles. *Inorg. Chem.* **2015**, *54*, 2713–2725.

(46) Sahu, K.; Mondal, S.; Patra, B.; Pain, T.; Patra, S. K.; Dosche, C.; Kar, S. Regioselective thiocyanation of corroles and the synthesis of gold nanoparticle–corrole assemblies. *Nanoscale Adv.* **2020**, *2*, 166–170.

(47) Ban, Y. L.; Dai, J. L.; Jin, X. L.; Zhang, Q. B.; Liu, Q. Thiocyanate radical mediated dehydration of aldoximes with visible light and air. *Chem. Commun.* **2019**, *55*, 9701–9704.

(48) Barber, D. C.; Freitag-Beeston, R. A.; Whitten, D. G. Atropisomer-specific formation of premicellar porphyrin J-aggregates in aqueous surfactant solutions. *J. Phys. Chem.* **1991**, *95*, 4074–4086.

(49) Zipp, C. F.; Michael, J. P.; Fernandes, M. A.; Marques, H. M. The synthesis and characterization of several corroles. *S. Afr. J. Chem.* **2013**, *66*, 158–166.

(50) Thomas, K. E.; Alemayehu, A. B.; Conradie, J.; Beavers, C.; Ghosh, A. Synthesis and Molecular Structure of Gold Triarylcorroles. *Inorg. Chem.* **2011**, *50*, 12844–12851.

(51) Rabinovich, E.; Goldberg, I.; Gross, Z. Gold (I) and gold (III) corroles. *Chem. - Eur. J.* **2011**, *17*, 12294–12301.

(52) Schmidbaur, H.; Raubenheimer, H. G.; Dobrzańska, L. The gold–hydrogen bond, Au–H, and the hydrogen bond to gold, Au···H–X. *Chem. Soc. Rev.* **2014**, *43*, 345–380.

(53) Rigoulet, M.; Massou, S.; Sosa Carrizo, E. D.; Mallet-Ladeira, S.; Amgoune, A.; Miqueu, K.; Bourissou, D. Evidence for genuine hydrogen bonding in gold (I) complexes. *Proc. Natl. Acad. Sci. U. S. A.* **2019**, *116*, 46–51.

(54) Kumar, M.; Francisco, J. S. Evidence of the Elusive Gold-Induced Non-Classical Hydrogen Bonding in Aqueous Environments. *J. Am. Chem. Soc.* **2020**, *142*, 6001–6006.

(55) Schmidbaur, H. Proof of Concept for Hydrogen Bonding to Gold, Au···H–X. *Angew. Chem., Int. Ed.* **2019**, *58*, 5806–5809.

(56) Hashimoto, T.; Choe, Y.-K.; Nakano, H.; Hirao, K. Theoretical study of the Q and B bands of free-base, magnesium, and zinc porphyrins, and their derivatives. *J. Phys. Chem. A* **1999**, *103*, 1894–1904.

(57) Shipman, L. L.; Cotton, T. M.; Norris, J. R.; Katz, J. J. An analysis of the visible absorption spectrum of chlorophyll a monomer, dimer, and oligomers in solution. *J. Am. Chem. Soc.* **1976**, *98*, 8222–8230.

(58) Romero, N. A.; Nicewicz, D. A. Organic photoredox catalysis. *Chem. Rev.* **2016**, *116*, 10075–10166.

(59) Schweyen, P.; Brandhorst, K.; Wicht, R.; Wolfram, B.; Bröring, M. The corrole radical. *Angew. Chem.* **2015**, *127*, 8331–8334.

(60) Bakar, M. A.; Sugiuchi, M.; Iwasaki, M.; Shichibu, Y.; Konishi, K. Hydrogen bonds to Au atoms in coordinated gold clusters. *Nat. Commun.* **2017**, *8*, 576.